Micro-SPECT/CT–Based Pharmacokinetic Analysis of ^{99m}Tc-Diethylenetriaminepentaacetic Acid in Rats with Blood–Brain Barrier Disruption Induced by Focused Ultrasound

Feng-Yi Yang[1], Hsin-Ell Wang[1], Guan-Liang Lin[1], Ming-Che Teng[1], Hui-Hsien Lin[1], Tai-Tong Wong[2], and Ren-Shyan Liu[1,3,4]

[1]Department of Biomedical Imaging and Radiological Sciences, National Yang-Ming University, Taipei, Taiwan; [2]Department of Neurosurgery, Neurological Institute, Veterans General Hospital, Taipei, Taiwan; [3]Department of Nuclear Medicine, National PET/Cyclotron Center, Taipei Veterans General Hospital, Taipei, Taiwan; and [4]Molecular and Genetic Imaging Core, National Yang-Ming University Medical School, Taipei, Taiwan

This study evaluated the pharmacokinetics of ^{99m}Tc-diethylenetriamine pentaacetate acid (^{99m}Tc-DTPA) after intravenous administration in healthy and F98 glioma–bearing F344 rats in the presence of blood–brain barrier disruption (BBB-D) induced by focused ultrasound (FUS). The pharmacokinetics of the healthy and tumor-containing brains after BBB-D were compared to identify the optimal time period for combined treatment. **Methods:** Healthy and F98 glioma–bearing rats were injected intravenously with Evans blue (EB) and ^{99m}Tc-DTPA; these treatments took place with or without BBB-D induced by transcranial FUS of 1 hemisphere of the brain. The permeability of the BBB was quantified by EB extravasation. Twelve rats were scanned for 2 h to estimate uptake of ^{99m}Tc radioactivity with respect to time for the pharmacokinetic analysis. Terminal deoxynucleotidyl transferase-mediated dUTP nick-end labeling (TUNEL) staining was performed to examine tissue damage. **Results:** The accumulations of EB and ^{99m}Tc-DTPA in normal brains or brains with a tumor were significantly elevated after the intravenous injection when BBB-D was induced. The disruption-to-nondisruption ratio of the brains and the tumor–to–ipsilateral brain ratio of the tumors in terms of radioactivity reached a peak at 45 and 60 min, respectively. EB injection followed by sonication showed that there was an increase of about 2-fold in the tumor–to–ipsilateral brain EB ratio of the target tumors (7.36), compared with the control tumors (3.73). TUNEL staining showed no significant differences between the sonicated tumors and control tumors. **Conclusion:** This study demonstrates that ^{99m}Tc-DTPA micro-SPECT/CT can be used for the pharmacokinetic analysis of BBB-D induced by FUS. This method should be able to provide important information that will help with establishing an optimal treatment protocol for drug administration after FUS-induced BBB-D in clinical brain disease therapy.

Key Words: focused ultrasound; blood–brain barrier disruption; ^{99m}Tc-DTPA; micro-SPECT; pharmacokinetics

J Nucl Med 2011; 52:478–484
DOI: 10.2967/jnumed.110.083071

Received Sep. 7, 2010; revision accepted Nov. 18, 2010.
For correspondence or reprints contact: Feng-Yi Yang, Department of Biomedical Imaging and Radiological Sciences, School of Biomedical Science and Engineering, National Yang-Ming University, Taipei, Taiwan.
E-mail: fyyang@ym.edu.tw

The blood–brain barrier (BBB) is mainly composed of endothelial cells that are closely linked by intercellular tight junctions. This barrier plays a key role in controlling the delivery of therapeutic agents to the brain (*1*). Advances in neuroscience have resulted in the development of new drugs and gene-based therapies that may be useful when treating many central nervous system diseases, but achieving a therapeutic level of these entities is often restricted by the BBB (*2–4*). Malignant glioma remains one of the most deadly types of tumor in humans, and patients have a poor prognosis even after radiation therapy and chemotherapy. To improve the life expectancy of these patients, new therapeutic techniques are vital. The basic concept of a binary system for tumor treatment is to locally destroy malignant cells while sparing normal tissues (*5,6*). Boron neutron capture therapy (BNCT) is one such binary tumor treatment and is based on a selective accumulation of ^{10}B in tumors while maintaining low levels in the surrounding normal tissues; the tumor is then irradiated to a sufficient level using a neutron source. For successful BNCT, a relatively high concentration of boron must be delivered to the tumor. Selective delivery of ^{10}B to a brain tumor is one of the key requirements of BNCT brain tumor treatment and is impeded by 2 obstacles, the BBB and the blood–tumor barrier (BTB). Notwithstanding the fact that the integrity of the BBB is often reduced somewhat near a brain tumor, antitumor agents are rarely effective in patients with brain tumors because the selective permeability of the BTB still stops the agent from reaching the target (*7,8*). Therefore, to ensure the efficacy of BNCT, it is important to explore the pharmacokinetics and relative concentrations of boron compounds in the brain for each patient before neutrons are irradiated.

Chemotherapy accompanied by biochemical or intracarotid perfusion of hyperosmotic mannitol has been used to induce a moderate augmentation of the drug delivery into the brain (*9–11*). Our previous study demonstrated that the concentration of boron in tumors and the tumor–to–normal

brain ratio of boron in the brain after BBB disruption (BBB-D) by mannitol injection are significantly higher than those without BBB-D (*12*). Nevertheless, this approach produces nonfocal BBB-D across the entire brain area supplied by the injected artery branch (*2,13*). Focused ultrasound (FUS) has been shown to locally and noninvasively increase the permeability of the BBB, and it has been found that these changes to the BBB are affected by various ultrasound parameters as well as by the dose of ultrasound contrast agent (UCA; SonoVue [Bracco International]) (*14–16*). A recent study has shown that treatment with FUS before drug administration can control tumor progression and improve animal survival (*17*). The purpose of this study was to investigate the pharmacokinetics of ^{99m}Tc-diethylenetriaminepentaacetic acid (^{99m}Tc-DTPA) after intravenous injection in healthy rats and into a glioma-bearing rat model when FUS-induced BBB-D was applied. Our results should help with the optimization of the treatment protocols for the binary treatment of brain disease.

MATERIALS AND METHODS

Tumor Model and Animal Preparation

All procedures were performed according to the guidelines and approved by the Animal Care and Use Committee of the National Yang-Ming University. Thirty-four Fischer 344 rats (9–12 wk old; ~290–340 g) were used in this work. Eighteen male Fischer 344 rats were anesthetized by an intraperitoneal administration of pentobarbital at a dose of 40 mg/kg of body weight. Then, 1×10^5 F98 rat glioma cells in 10 μL of Hanks' balanced salt solution without Mg^{2+} and Ca^{2+} were injected into the brains of these rats. The glioma cells were stereotactically injected into a single location in the hemispheres (5.0 mm posterior and 3.0 mm lateral to the bregma) of each rat at a depth of 5.0 mm from the brain surface. Next, the holes in the skull were sealed with bone wax, and the wound was flushed with iodinated alcohol. All glioma-bearing rats were sonicated by FUS targeting the right brain hemisphere on day 8 after tumor cell implantation. Nine glioma-bearing rats were assessed by Evans blue (EB) extravasation for BBB permeability. Six glioma-bearing rats were used for SPECT/CT to evaluate the pharmacokinetics of ^{99m}Tc-DTPA. Three glioma-bearing rats were histologically examined using terminal deoxynucleotidyl transferase-mediated dUTP nick-end labeling (TUNEL) staining. Furthermore, 16 healthy rats were used to evaluate BBB permeability and monitor the pharmacokinetics of ^{99m}Tc-DTPA after BBB-D in the normal brain.

FUS System and Sonication

Pulsed-FUS exposures were performed with a single-element focused transducer (A392S; Panametrics) (diameter, 38 mm; radius of curvature, 63.5 mm; and resonant frequency, 1.0 MHz). The shape of the focal zone of the therapeutic transducer was an elongated ellipsoid, with a radial diameter (–6 dB) of 3 mm and an axial length (–6 dB) of 26 mm. The whole transducer driving system is similar to that used in our previous work (*18*).

UCA was injected into the femoral vein of the rats about 15 s before each sonication. The agent contained phospholipid-coated microbubbles at a concentration of $1–5 \times 10^8$ bubbles/mL, with the bubbles having a mean diameter of 2.5 μm. The FUS exposure was precisely targeted using a stereotactic apparatus (Stoelting) that used the bregma of the skull as the anatomic landmark. The FUS beam was delivered to 1 location in the right brain hemisphere centered on the tumor injection site. The following sonication parameters were used: an acoustic power of 5.72 W with an injection of 300 μL of UCA per kilogram, a pulse repetition frequency of 1 Hz, and a duty cycle of 5% (50 ms on, and 950 ms off).

MRI

MRI was performed using a 3-T system (Magnetom Trio 3-T MRI; Siemens) after FUS sonication. The rats were anesthetized with isoflurane mixed with oxygen during the imaging procedure. A loop coil (Loop Flex Coil [Siemens], ~4 cm in diameter) for radiofrequency reception was used. A multislice spin-echo sequence, covering the whole brain to depict the BBB-D (repetition time/echo time, 500/13; matrix, 243 × 512; section thickness, 1.0 mm), was performed to obtain 20 slices of the T1-weighted MR image. The imaging plane was located across the focus at the focal depth. An MRI contrast agent, gadolinium (Omniscan; GE Healthcare), was injected (1 mmol/kg) intravenously at 5 min before sonication. Subsequently, MRI contrast enhancement was analyzed at 30 min after sonication for a normal rat brain.

Evaluation of BBB Integrity

BBB integrity can be quantified on the basis of the extravasation of EB, which acts as a marker of albumin extravasation (*15,18,19*). EB (Sigma) (100 mg/kg) was injected intravenously about 5 min before FUS exposure. Animals were euthanized with an overdose of pentobarbital at approximately 30 min after the sonication. After perfusion and brain removal, the normal brain was sectioned into 3 slices (6 mm posterior to the bregma) and mounted on glass slides. In addition to this processing, the hemispheres of the glioma-bearing brains were dissected into tumor tissue and normal brain tissue before the amount of EB extravasation was measured. The left unsonicated brains acted as the controls. Samples were weighed and then soaked in 50% trichloroacetic acid solution. After homogenization and centrifugation, the extracted dye was diluted with ethanol (1:3) and the amount of dye present measured using a spectrophotometer (PowerWave 340; BioTek) at 620 nm. The EB present in the tissue samples was quantified using a linear regression standard curve derived from 7 concentrations of the dye; the amount of dye is denoted in absorbance per gram of tissue.

SPECT/CT

A FLEX Triumph preclinical imaging system (Gamma Medica-Ideas, Inc.) was used for the small-animal SPECT/CT scan acquisition. This system applied circular scanning protocols for both SPECT and CT acquisition, with a translation stage in a variable axial imaging range. The axial field of view for CT without stage translation was 61.44 mm. The CT system had a power-adjustable 10-ray emitter ranging from 50 to 80 kVp and a microfocus (<50 μm) tube. Each rat was injected intravenously with a 74-MBq (2 mCi)/0.5 cm^3 concentration of ^{99m}Tc-DTPA at 25 min after sonication. The SPECT projection dataset was acquired using 3 low-energy, high-resolution pinhole collimators with a radius of rotation of 50 mm. The rats were anesthetized by inhalation of isoflurane with oxygen and were scanned first by CT using 512 slides for anatomic coregistration and then by a dynamic SPECT sequence involving 8 frames. Thirty-two projections (28 s) were acquired over 180°, and these formed a 60 × 60 matrix, which needed a total imaging time of 15 min per frame. The image dataset was then reconstructed using the ordered-subset

expectation maximization algorithm with standard-mode parameters as provided by the manufacturer. No scatter or attenuation correction was applied to the reconstructed images. Pinhole SPECT images of a standard amount of radioactivity were acquired as a reference for quantification, and decay was corrected using radioactivity counts measured with a γ-counter (VDC-405; Veenstra Instruments). The uptake of ^{99m}Tc-DTPA by the various tissues was expressed as a percentage of the injected dose per milliliter of tissue.

The images were viewed and quantified using AMIDE software (*20*) (free software provided by SourceForge). Cylindric regions of interest (2 × 2 × 2 mm) under the skull defect were manually pinpointed at the sonicated site and in the same region of the contralateral brain. The image counts within the regions of interest were converted to absolute radioactivity using an efficiency factor determined from the reference standard radioactivity. The mean radioactivities within the regions of interest were converted to injected dose per milliliter of tissue to normalize relative to the total injected dose. The radioactivities within the BBB-D region at different times were determined and compared with the results obtained from the equivalent contralateral brain region.

Histologic Observations

Three glioma-bearing rats were perfused with saline and 10% neutral-buffered formalin at about 4 h after sonication. The brains were removed and embedded in paraffin and then serially sectioned into 6-μm-thick slices. The slices were stained by TUNEL (DeadEnd Colorimetric TUNEL system, G7130; Promega) to detect DNA fragmentation and apoptotic bodies within the cells (*21*). The histologic examination was performed by light microscopy (Olympus BX61; Olympus). The total area of each tissue section and the areas showing apoptosis were measured using the Image-Pro Plus software (Media Cybemetics) in a masked manner. The percentage of the tissue with apoptosis was calculated as follows: (area of the tissue that is damaged with apoptotic cells/total area of the tissue sections measured) × 100. Six tissue sections from each brain were analyzed for each animal.

Statistical Analysis

All values are shown as mean ± SEM. Statistical analysis was performed using an unpaired Student *t* test. Statistical significance was defined as a *P* value of 0.05 or less.

RESULTS

The rats' mean body weights were greatest immediately after tumor cell implantation and decreased as a function of time due to growth of the tumor. Compared with the first day after tumor implantation, the mean body weight was significantly decreased on day 8. BBB permeability was therefore evaluated in glioma-bearing brains on day 8 after implantation; both glioma-bearing and contralateral hemispheres were examined. BBB-D, as indicated by EB extravasation, was observed in the focal zone of the FUS beam.

Figures 1A and 1B show the average extravasation of EB (in μg/g of tissue) and the disruption-to-nondisruption EB ratios in normal brains injected intravenously with EB immediately and at 48 h after sonication. Figures 1C and 1D show the average extravasation of EB (in μg/g of tissue) and the tumor-to-ipsilateral brain EB ratios in the glioma-bearing brains injected intravenously with EB immediately and at 48 h after sonication. In both cases, the degree of EB extravasation in the right sonicated brain was significantly greater than in the left control brain. Furthermore, in both cases BBB integrity (Fig. 1A, $P = 0.24$) and BTB (Fig. 1C, $P = 0.56$) appeared to have been reestablished at 48 h because administration of EB at this time led to no difference between the sonicated site and its control site.

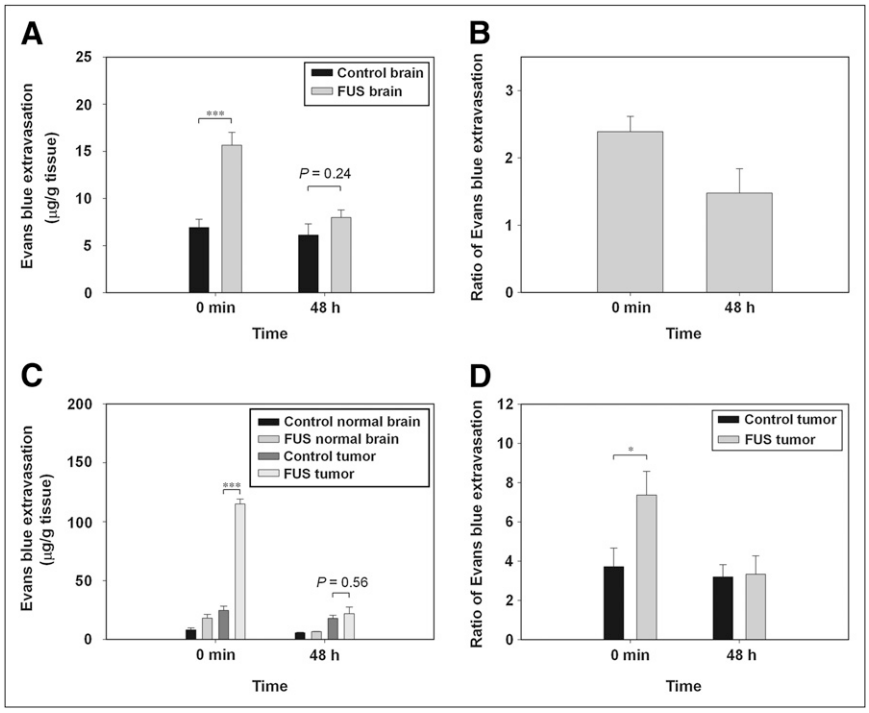

FIGURE 1. Immediately after and at 48 h after sonication, EB extravasation was measured in brain tissue. (A) EB in sonicated and contralateral regions of normal brain. (B) Disruption–to–nondisruption ratio of normal brain. (C) EB in tumor tissue and in neighboring normal brain regions with and without sonication. Immediately after sonication, EB in brain tumor with sonication was significantly higher than that in brain tumor without sonication. No significant difference was found between them at 48 h after sonication. (D) Tumor–to–ipsilateral brain EB ratio of brain tumor. *$P < 0.05$. ***$P < 0.001$.

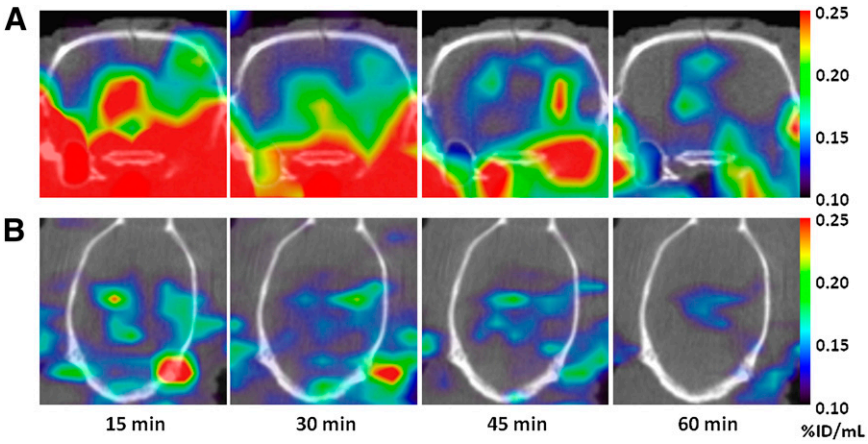

FIGURE 2. SPECT/CT images of F98 glioma–bearing Fischer 344 rats at 15, 30, 45, and 60 min after intravenous injection of 74 MBq (2 mCi) of ^{99m}Tc-DTPA in axial (A) and coronal (B) views. Right brain, tumor with sonication; left brain, tumor without sonication. Animals were under isoflurane anesthesia, and image acquisition time was 15 min.

The animal SPECT images showed a limited uptake of radioactivity by the normal brain only, and this limited uptake contrasts with the intense uptake of radioactivity by the salivary glands. This biodistribution of ^{99m}Tc-DTPA is consistent with previous studies (*22*). BBB-D in the right sonicated hemisphere can be clearly seen in terms of uptake of ^{99m}Tc-DTPA at 30 and 45 min after injection. In the micro-SPECT/CT scan of the glioma-bearing rats, high contrast between the sonicated tumor and control tumor can be seen at 30 and 45 min after the injection of ^{99m}Tc-DTPA (Fig. 2).

A significant extravasation of radioactivity can be seen in the BBB-D regions of the right striatum. The accumulation of ^{99m}Tc-DTPA at the sonicated site and the disruption-to-nondisruption ratio of the brains in normal Fischer 344 rats reached a maximum value at 45 min after injection (Fig. 3). The time–activity curves for ^{99m}Tc-DTPA in the tumor and ipsilateral brain derived from the dynamic SPECT images are shown in Figure 4A. The uptake of ^{99m}Tc-DTPA by the tumors is significantly greater after FUS sonication. The derived tumor-to-ipsilateral brain ratios after ^{99m}Tc-DTPA administration (Fig. 4B) show a peak value of about 2.0 at 60 min after intravenous injection and BBB-D by FUS. In contrast to the ratio for the sonicated tumors, only insignificant differences were found for the control tumor ratios across various time points.

No significant difference in apoptosis between the sonicated tumors and control tumors was found (Fig. 5). From histologic examination, the regions of apoptotic cells were heterogeneously distributed across the tumors. Cell apoptosis was also found in brain regions adjacent to the great vessels and in areas near the skull.

DISCUSSION

Previous work has shown that MRI can be used to monitor the degree of BBB-D and to analyze the spatiotemporal distribution of BBB-D when it is induced by FUS (*23,24*). However, these studies have provided little information on the pharmacokinetics of model drug delivery. ^{99m}Tc-DTPA shares the same pharmacokinetics of MRI contrast agent and is the first choice for the evaluation of BBB-D (*25*). In the present study, we investigated the pharmacokinetics in normal and tumor-bearing brains after intravenous injection of ^{99m}Tc-DTPA with or without BBB-D using a noninvasive method. The results showed that the accumulation of radioactivity in the sonicated brain tumors after BBB-D was higher than that for the control groups, suggesting that SPECT and radiolabeled drugs might be a useful approach to noninvasively assessing the pharmacokinetics of BBB-D during sonication.

^{99m}Tc-DTPA has been widely used to detect changes in BBB permeability in humans in studies of various clinical applications. However, only a few studies have investigated whether ^{99m}Tc-DTPA can be used as a tracer to measure BBB permeability in animals. Because the mean brain volume of the rat is only about 1 cm^3 in our study, the biodistribution of ^{99m}Tc-DTPA in the normal brain after injection was approximately 0.1% injected dose (Figs. 3A and 4A). This value is in keeping with values found previously (*22*). The accumulation of ^{99m}Tc-DTPA after intravenous administration in sonicated brains or in sonicated tumors, when BBB-D has occurred, showed a reasonable delay relative to the absorption phase. The time to maximum radioactivity was 45 min in the sonicated brains and 30 min in tumors when there has been BBB-D. Figure 1 shows that permeability is higher for tumors with BBB-D than for sonicated brain without a tumor. This may be the reason why tumors with BBB-D take a shorter time to reach the peak of radioactivity. According to the quantitative SPECT data, compared with the contralateral and ipsilateral brains (Figs. 3B and 4B), the disruption-to-nondisruption ratio for normal brains and the tumor–to–ipsilateral brain ratio for tumor-containing brains in terms of radioactivity showed a 1.43- and 2.00-fold increase, respectively. However, as measured by EB extravasation immediately after sonication, the disruption-to-nondisruption ratio of the normal brain and the tumor–to–ipsilateral brain ratio for tumor-containing brains are 2.39- and 7.36-fold increased, respectively (Figs. 1B and 1D). Thus, the noninvasive ^{99m}Tc-DTPA SPECT approach seems to yield only a relative rather than an absolute quantification index across the various time points.

Various investigations have demonstrated that when the brain is exposed to FUS, there is a transient and reversible

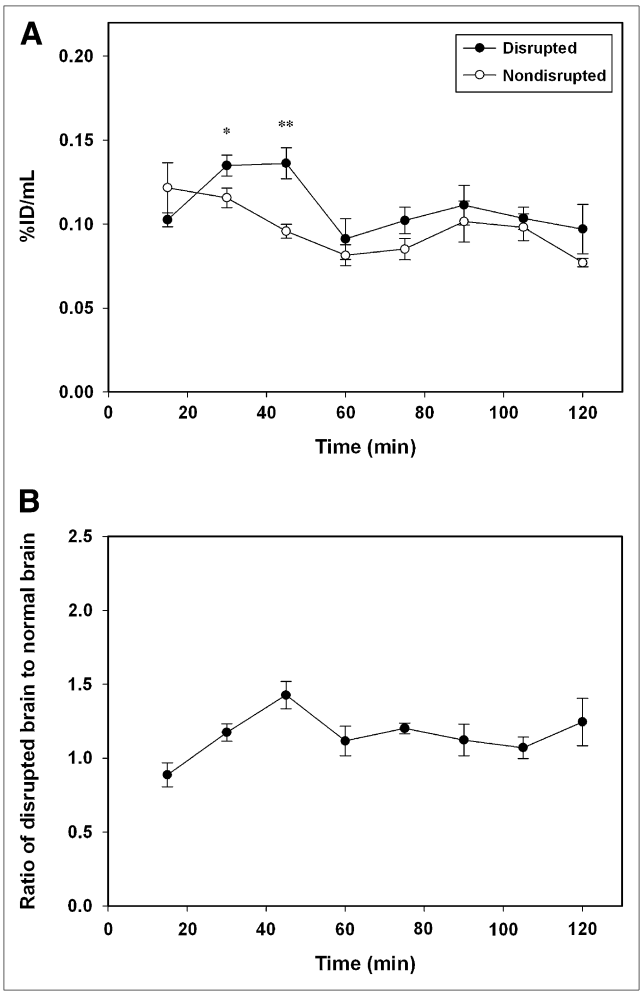

FIGURE 3. Pharmacokinetics of ^{99m}Tc-DTPA for normal Fischer 344 rats was determined by SPECT/CT. (A) Time–activity curves of ^{99m}Tc-DTPA in sonicated and contralateral brains of Fischer 344 rats were derived from dynamic SPECT/CT images after intravenous injection; these were measured with and without BBB-D. (B) Disruption-to-nondisruption ratios of ^{99m}Tc-DTPA in brains. $^{*}P < 0.05$. $^{**}P < 0.01$.

opening of the BBB (*18*). In a similar way to that found for FUS-induced BBB-D, Figures 1C and 1D show that FUS-enhanced BTB permeability is also transient because EB extravasation at the sonicated tumor site was approximately the same as for the control tumor at 48 h after sonication. Moreover, no significant differences in the distribution of apoptotic cells were found between FUS-exposed tumors and control tumors (Fig. 5). BBB-D was therefore evaluated in glioma-bearing brains after sonication at an acoustic power of 5.72 W with an injection of 300 μL of UCA per kilogram. It would appear that changes in BBB-D in the ipsilateral brain with or without sonication would show the same effect as the normal-brain studies (Figs. 1A and 1C). Pulsed high-intensity focused ultrasound also obviously enhanced permeability in the normal brain tissue surrounding the sonicated tumor. Nevertheless, the enhanced uptake in the tumor tissue, although sparing the normal tissue, would be practicable when treating tumors using a phased-array transducer with strong focused ultrasound beam.

In addition to tracking the EB distribution, we also monitored gadolinium deposition and the pattern of contrast enhancement in the sonicated normal brain by signal intensity level. The pattern of contrast enhancement after the FUS beam has targeted the brain tissue does not correspond to the circular pattern of the ultrasound beam at the cross section of focus (not shown). The irregularity of the contrast enhancement is similar to that found in a previous study (*24*). Additionally, MR images also show significant enhancement at the bottom of the brain, which can be seen in the MR images as well as in the EB-stained specimens. This enhancement may be because there is an acoustic impedance mismatch at the brain–bone interface that leads to strong acoustic reflection from the bottom of the brain.

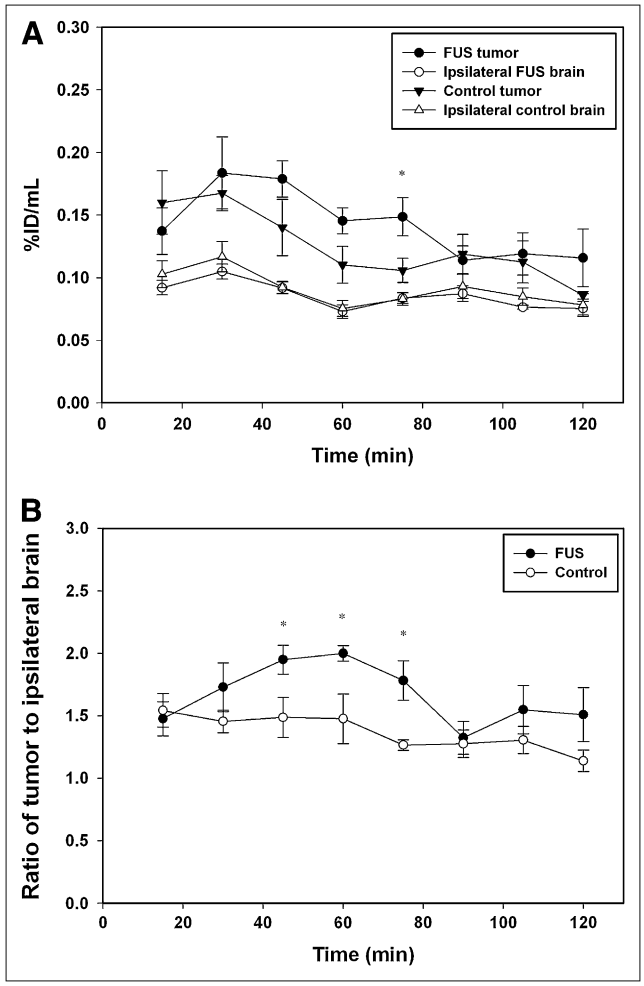

FIGURE 4. Pharmacokinetics of ^{99m}Tc-DTPA for F98 glioma–bearing rats determined by SPECT/CT. (A) Time–activity curves of ^{99m}Tc-DTPA in tumors and in ipsilateral brains of F98 glioma–bearing rats were derived from dynamic SPECT/CT images after intravenous injection; these were measured with and without BBB-D. (B) Tumor–to–ipsilateral brain ratio for ^{99m}Tc-DTPA. $^{*}P < 0.05$.

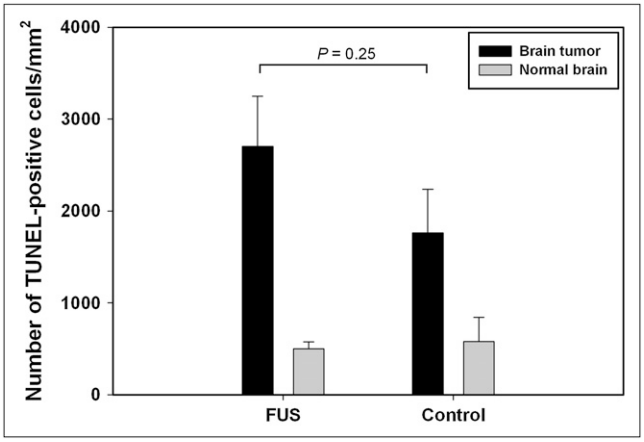

FIGURE 5. Numbers of apoptotic cells (mean ± SEM) in sonicated tumors and control tumors from histologic observations using TUNEL-stained sections.

For BNCT, the main factors affecting effectiveness are the thermal neutron flux and the boron concentration within the tumor. Enhancing the delivery of boron to a tumor by FUS may be a useful way to optimize BNCT. Our previous study has shown that intracarotid administration of hypertonic mannitol, which results in BBB-D, not only significantly increased the accumulation of boron drugs in the brain tumor, compared with the results without BBB-D, but also elevated significantly the tumor-to-brain ratio (*12*). The present research shows that completely noninvasive focal disruption of the BTB, which can be induced by FUS, is able to enhance the ^{99m}Tc-DTPA concentration in the tumor and the tumor-to-brain ratio across the tumor-containing brain. Therefore, it should be possible to identify an optimal time between administration of the neutron capture agent and neutron irradiation based on the differential uptake of boron between tumor and normal tissues after FUS exposure. The results of this pilot study therefore suggest that a further evaluation using other radiotracers is warranted. One possibility is a 4-borono-2-^{18}F-fluoro-L-phenylalanine PET study of the pharmacokinetics of L-*p*-boronophenylalanine after BBB-D. This type of study may be advantageous in terms of nuclear image scanning and provide a suitable tool for monitoring the drug distribution. Such investigations will allow the identification of an optimal therapeutic window when using FUS sonication as part of a treatment regimen.

CONCLUSION

^{99m}Tc-DTPA micro-SPECT/CT shows that FUS not only significantly increases the permeability of the BBB at the sonicated site but also significantly elevates the lesion–to–normal brain ratio in the focal region. This noninvasive approach offers a good assessment of the extent of BBB-D and may be useful as a way of identifying an optimal window for effective BNCT or other brain disease treatments that will have minimal negative side effects.

ACKNOWLEDGMENTS

This study was supported by grants from the National Science Council of Taiwan (NSC 99-2314-B-010-028 and NSC 99-2321-B-010-017), Yen Tjing Ling Medical Foundation (grant CI-99-8), the Department of Health of Taiwan (DOH99-TD-C-111-007), and the Ministry of Education "Aim for the Top University" Plan and was supported in part by the 3-T MRI Core Facility in National Yang-Ming University. This work also was supported (in part) by the Molecular and Genetic Imaging Core/National Research Program for Genomic Medicine at National Yang-Ming University.

REFERENCES

1. Bradbury MW. The structure and function of the blood-brain barrier. *Fed Proc.* 1984;43:186–190.
2. Abbott NJ, Romero IA. Transporting therapeutics across the blood-brain barrier. *Mol Med Today.* 1996;2:106–113.
3. Nag S. Morphology and molecular properties of cellular components of normal cerebral vessels. *Methods Mol Med.* 2003;89:3–36.
4. Pardridge WM. Drug and gene delivery to the brain: the vascular route. *Neuron.* 2002;36:555–558.
5. Slatkin DN. A history of boron neutron capture therapy of brain tumours: postulation of a brain radiation dose tolerance limit. *Brain.* 1991;114:1609–1629.
6. Barth RF, Soloway AH, Fairchild RG, Brugger RM. Boron neutron capture therapy for cancer: realities and prospects. *Cancer.* 1992;70:2995–3007.
7. Black KL, Ningaraj NS. Modulation of brain tumor capillaries for enhanced drug delivery selectively to brain tumor. *Cancer Control.* 2004;11:165–173.
8. Neuwelt EA. *Implications of the Blood-Brain Barrier and Its Manipulation*. New York, NY: Plenum; 1989.
9. Haluska M, Anthony ML. Osmotic blood-brain barrier modification for the treatment of malignant brain tumors. *Clin J Oncol Nurs.* 2004;8:263–267.
10. Kemper EM, Boogerd W, Thuis I, Beijnen JH, van Tellingen O. Modulation of the blood-brain barrier in oncology: therapeutic opportunities for the treatment of brain tumours? *Cancer Treat Rev.* 2004;30:415–423.
11. Sage MR, Wilcox J, Evill CA, Benness GT. Comparison and evaluation of osmotic blood-brain barrier disruption following intracarotid mannitol and methylglucamine iothalamate. *Invest Radiol.* 1982;17:276–281.
12. Hsieh C, Chen Y, Chen F, et al. Evaluation of pharmacokinetics of 4-borono-2-^{18}F-fluoro-L-phenylalanine for boron neutron capture therapy in a glioma-bearing rat model with hyperosmolar blood-brain barrier disruption. *J Nucl Med.* 2005;46:1858–1865.
13. Kroll RA, Neuwelt EA. Outwitting the blood-brain barrier for therapeutic purposes: osmotic opening and other means. *Neurosurgery.* 1998;42:1083–1099, discussion 1099–1100.
14. Hynynen K, McDannold N, Sheikov NA, Jolesz FA, Vykhodtseva N. Local and reversible blood-brain barrier disruption by noninvasive focused ultrasound at frequencies suitable for trans-skull sonications. *Neuroimage.* 2005;24:12–20.
15. Yang F, Fu W, Chen W, Yeh W, Lin W. Quantitative evaluation of the use of microbubbles with transcranial focused ultrasound on blood-brain-barrier disruption. *Ultrason Sonochem.* 2008;15:636–643.
16. Treat LH, McDannold N, Vykhodtseva N, Zhang Y, Tam K, Hynynen K. Targeted delivery of doxorubicin to the rat brain at therapeutic levels using MRI-guided focused ultrasound. *Int J Cancer.* 2007;121:901–907.
17. Liu HL, Hua MY, Chen PY, et al. Blood-brain barrier disruption with focused ultrasound enhances delivery of chemotherapeutic drugs for glioblastoma treatment. *Radiology.* 2010;255:415–425.
18. Yang FY, Liu SH, Ho FM, Chang CH. Effect of ultrasound contrast agent dose on the duration of focused-ultrasound-induced blood-brain barrier disruption. *J Acoust Soc Am.* 2009;126:3344–3349.
19. Yang F, Fu W, Yang R, Liou H, Kang K, Lin W. Quantitative evaluation of focused ultrasound with a contrast agent on blood-brain barrier disruption. *Ultrasound Med Biol.* 2007;33:1421–1427.

20. Loening AM, Gambhir SS. AMIDE: a free software tool for multimodality medical image analysis. *Mol Imaging.* 2003;2:131–137.
21. Gavrieli Y, Sherman Y, Ben-Sasson SA. Identification of programmed cell death in situ via specific labeling of nuclear DNA fragmentation. *J Cell Biol.* 1992; 119:493–501.
22. Prato FS, Wisenberg G, Marshall TP, Uksik P, Zabel P. Comparison of the biodistribution of gadolinium-153 DTPA and technetium-99m DTPA in rats. *J Nucl Med.* 1988;29:1683–1687.
23. Hynynen K, McDannold N, Vykhodtseva N, Jolesz FA. Noninvasive MR imaging-guided focal opening of the blood-brain barrier in rabbits. *Radiology.* 2001;220:640–646.
24. Choi JJ, Pernot M, Brown TR, Small SA, Konofagou EE. Spatio-temporal analysis of molecular delivery through the blood-brain barrier using focused ultrasound. *Phys Med Biol.* 2007;52:5509–5530.
25. Loberg MD, Corder EH, Fields AT, Callery PS. Membrane transport of Tc-99m-labeled radiopharmaceuticals, I. Brain uptake by passive transport. *J Nucl Med.* 1979;20:1181–1188.